Polymer 49 (2008) 3902–3910

Contents lists available at ScienceDirect

Polymer

journal homepage: www.elsevier.com/locate/polymer

Synthesis and characterization of TPO–PLA copolymer and its behavior as compatibilizer for PLA/TPO blends

Chang-Hong Ho [a], Chau-Hui Wang [b], Chin-I Lin [b], Yu-Der Lee [a,*]

[a] Department of Chemical Engineering, National Tsing Hua University, Hsinchu, 30013, Taiwan
[b] Industrial Technology Research Institute, Hsinchu, 30013, Taiwan

ARTICLE INFO

Article history:
Received 18 March 2008
Received in revised form 24 June 2008
Accepted 27 June 2008
Available online 6 July 2008

Keywords:
TPO–PLA copolymer
Compatibilizer
Toughness

ABSTRACT

A thermoplastic polyolefin elastomer-*graft*-polylactide (TPO–PLA) was prepared by grafting polylactide onto maleic anhydride-functionalized TPO (TPO–MAH) in the presence of 4-dimethylaminopyridine (DMAP). The characterization of the TPO–PLA copolymers was conducted by FT-IR and ^{1}H NMR. The effects of reaction temperature and concentration of DMAP on the reactivity of graft polymerization were investigated by FT-IR, which revealed that a high reaction temperature and a high DMAP concentration are associated with dramatic depolymerization of PLA and reduction of steric hindrance effect in the graft reaction. A Molau test, SEM observations of cyro-fractured surface morphology and particle size analysis of PLA/TPO blend system demonstrate that this new copolymer, acting as a premade compatibilizer, significantly improved the compatibility of the PLA/TPO blends. As the concentration of TPO–PLA copolymer increased, elongation at break and tensile toughness increased with compatibilizer concentration up to 2.5 wt%, beyond which it declined, but TPO–PLA copolymer did not affect the tensile strength or modulus. The effect of the chemical composition of the TPO–PLA copolymer on the compatibilization efficiency and mechanical properties of the PLA/TPO blends was examined by altering the number of grafting sites and concentration of DMAP, suggesting that DMAP concentration dominated the properties of the ternary blend system. Two compatibilizers, TPO–MAH and TPO–PLA, were used to compatibilize the PLA/TPO blend; the results suggested that TPO–PLA was more efficient in reducing the interfacial tension between the two immiscible polymers and in improving the mechanical properties of PLA/TPO blending specimens.

1. Introduction

Polylactide (PLA), a synthetic aliphatic polyester derived from biomasses, is an environmentally friendly polymer and has been emerging as an alternative to conventional petroleum-based polymeric materials because of its renewability, biodegradability and greenhouse gas neutrality. PLA is most commonly synthesized by the ring opening polymerization of lactide, which is the cyclic dimer of lactic acid. The chirality of the three stereoisomers – L-lactide, D-lactide and D,L-lactide, substantially dominates the properties of PLA: poly(L-lactide) (PLLA) or poly(D-lactide) (PDLA) with high optical purity is semicrystalline with a T_m of 170–180 °C and a T_g of 55–65 °C, and amorphous poly(D,L-lactide) (PDLLA) only has a T_g of 50–60 °C.[1,2] Although PLA is a high-strength and high-modulus polymer analogous to polystyrene, its inherent brittleness and low toughness due to the low entanglement density (V_e) and the high value of characteristic ratio that represents the chain stiffness [3,4] restrict the range of applications.

Among various methods for modifying PLA, such as the copolymerization of lactide with other monomers, blending PLA with immiscible or miscible polymers is a more practical and economical way of toughening PLA [5–8]. However, most of the polymer blends are immiscible, and the multiphase blends show poor mechanical performance because of the low interfacial adhesion between the polymer phases. To solve the problem of immiscibility, compatibilizing agents, such as (i) premade block or graft copolymers that bear constitutive segments that are miscible with the blend components [9,10], or (ii) polymers with complementary reactive groups that can link the matrix with the dispersed phase via covalent bonds formed *in situ* during melt blending process, are utilized to reduce the interfacial tension and elevate interface adhesion between the immiscible phases [11,12].

Poly(ethylene-octene) copolymer is a thermoplastic polyolefin elastomer (TPO), and has been extensively employed as a toughening agent in numerous polymer blending systems, including polyester [13–15], and nylon [16]. These polymer blends, inclusive of PLA/TPO blend, are immiscible due to the high polarity difference between the component polymers. Hillmyer et al. [17,18] synthesized polyethylene-*block*-polylactide and poly(ethylene-*alt*-propylene)-*block*-polylactide via a combination of the anionic

* Corresponding author. Tel.: +886 3 5713204; fax: +886 3 5715408.
E-mail address: ydlee@che.nthu.edu.tw (Y.-D. Lee).

0032-3861/$ – see front matter © 2008 Elsevier Ltd. All rights reserved.
doi:10.1016/j.polymer.2008.06.054

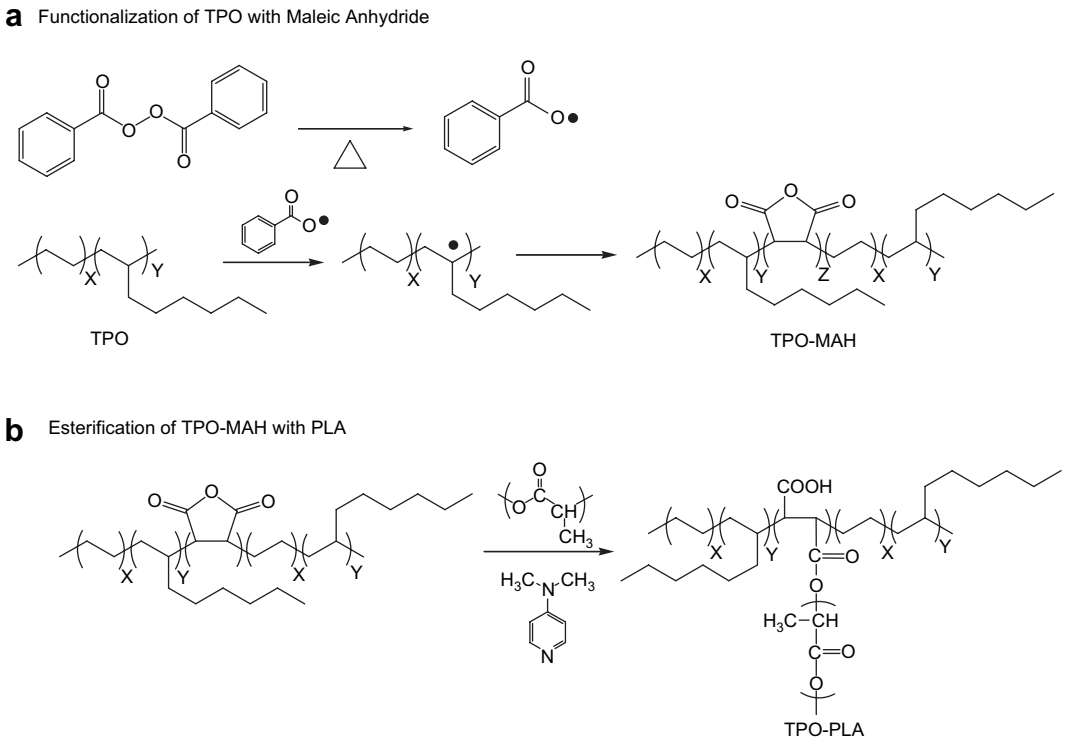

Scheme 1. The synthetic route of TPO–PLA copolymer.

polymerization of butadiene and isoprene and the ring opening polymerization of lactide; they demonstrated that these block copolymers were good compatibilizers for PLLA/LDPE blends. However, ionic polymerization and ring opening polymerization techniques suffer from the stringent requirement for moisture removal and monomer purity, and stannous octoate ($SnOct_2$) that is typically utilized in the PLA synthesis is not easily removed by dissolution and precipitation.

Over the past decades, considerable effort has been made to chemical modification of polyolefin by introducing reactive functional monomers to improve the properties and extend the range of applications of polyolefin, such as poly(polypropylene)-*g*-MAH [19], poly(ethylene)-*g*-MAH [20] and so on. The active functional group can react with numerous reactive groups to form block or graft copolymers acting as *in situ* formed or premade compatibilizers.

In this study, we report an alternative route for the preparation of TPO-*graft*-PLA copolymers that serve as compatibilizing agents for PLA/TPO blends: the maleic anhydride-functionalized TPO (TPO–MAH) reacts with the commercialized polylactide in the presence of 4-dimethylaminopyridine (DMAP). The chemical structures were identified by FT-IR and ^{1}H NMR. The factors influencing the reactivity of grafting PLA onto TPO were discussed. The morphologies and the mechanical properties of the PLA/TPO blends in the presence and absence of compatibilizers were studied, and the effect of the chemical composition of the TPO–PLA copolymers on the mechanical properties was analyzed and discussed. Finally, the mechanical properties and morphologies of PLA/TPO/TPO–MAH ternary blend were compared with those of PLA/TPO/TPO–PLA blend.

2. Experimental

2.1. Materials

PLA (NatureWorks 8300D) utilized in this study was purchased from Cargill–Dow Polymer LLC, and thermoplastic polyolefin elastomer (ENGAGE™ 8411) was obtained from Dow–Dupont elastomer. Acetone, ethyl acetate, and toluene, obtained from TEDIA; maleic anhydride (MAH) obtained from SHOWA; and benzoyl peroxide (BPO) obtained from Lancaster were all used as-received without further purification. 4-Dimethylaminopyridine (DMAP), purchased from Seedchem Company, was purified by recrystallization from toluene.

2.2. Preparation of TPO-graft-PLA copolymer

2.2.1. Functionalization of TPO with maleic anhydride

The reaction was conducted in a two-necked round-bottom flask equipped with a nitrogen gas inlet and a condenser and purged with dry-nitrogen gas. A desired amount of TPO pellets and MAH was added to the vessel, followed by injecting toluene into the flask and immersing the apparatus into an oil bath at 140 °C in sequence. After TPO and MAH were completely dissolved, BPO was added to the solution in an atmosphere of nitrogen. After the reaction mixture had been stirred for approximately 4 h, the reaction solution was poured into acetone to precipitate the functionalized polymer (TPO–MAH). TPO–MAH was further purified by HPLC-grade acetone by Soxhlet extraction overnight and was then dried at 80 °C at reduced pressure for 18 h.

2.2.2. Esterification of TPO–MAH with polylactide

TPO–MAH was added to a two-necked round-bottom flask equipped with a nitrogen gas inlet and a condenser. Toluene was injected and the reaction vessel was placed in an oil bath at 140 °C. After TPO–MAH was entirely dissolved, DMAP was added to the polymer solution. After the DMAP containing solution had been stirred for 1 h, the polylactide pellets were added and the graft reaction proceeded for 16 h. The final product was precipitated into ethyl acetate, and further purification by Soxhlet extraction with HPLC-grade ethyl acetate was accomplished, followed by drying in a vacuum oven at 80 °C for 18 h.

2.3. Characterization of TPO–MAH and TPO–PLA copolymer

The chemical structures of TPO–MAH and TPO–PLA were confirmed by nuclear magnetic resonance (NMR) and Fourier transformation infrared spectroscopy (FT-IR). ^{1}H NMR spectra were recorded on Varian Unityinova 500 NMR Spectrometer operated at 500 MHz at 60 °C, and d_8-toluene was used as solvent. The specimens for IR measurement were prepared by dissolving TPO–MAH and TPO–PLA in chloroform, coating the solution on a KBr pellet and drying in the convective oven. The IR spectra were recorded in the range of 4000 cm^{-1} and 400 cm^{-1} with a resolution of 2 cm^{-1}; and 16 scans were performed for each specimen.

The molecular weight of polylactide was determined by GPC with THF as solvent at a flow rate of 1 ml/min. The calibration curve was constructed based on polystyrene standards. The inherent viscosities of TPO-derived copolymers were measured at 35 °C with Ubbelohde capillary viscometer, and the concentration of each sample was 0.5 g/dL in toluene. The particle size of TPO in the PLA matrix was determined by dynamic light scattering instrument (Zetasizer Nano-S, model Zen1600). The specimens of the PLA/TPO blend were dissolved in ethyl acetate using sonicator to prevent the TPO particle from coalescence before the measurements were made.

2.4. Preparation of PLA/TPO blend

PLA/TPO blends were prepared in a Brabender mixer. Polylactide and TPO–PLA copolymer were dried in an oven at reduced pressure at 70 °C overnight before the melt blending to prevent polylactide from hydrolysis during the melt blending process. The weight ratio of PLA to TPO was maintained at 80:20, and the weight percentage of the TPO–PLA copolymer was varied from 0 wt% to 5 wt% of the total weight of the PLA/TPO blends. The premixed mixture of PLA and TPO pellets with or without TPO–PLA copolymer was introduced into the mixing chamber which was heated to 180 °C, and the blade rotated at a constant rate of 50 rpm. After 5 min, the PLA/TPO blends were removed from the mixing chamber, and the cooled chunks of PLA/TPO blends were ground into fine particles for further specimen preparation.

2.5. Molau test

A Molau test was performed to verify the formation of this graft copolymer and the compatibility of the polymer components: 0.1 g of the PLA/TPO (80/20) binary blend and the PLA/TPO/TPO–PLA (80/20/5) ternary blend were dissolved in 10 ml of ethyl acetate by ultrasonication. The mixture solution was left to stand for at least 24 h.

2.6. Preparation of specimens for mechanical property tests

All of the specimens used in the mechanical property test were manufactured by hot compression molding method: the weighed ground powders of PLA/TPO blends were added to the mold and pre-heated at 180 °C for 5 min; the polymer melts were then degassed and the melt blends were molded at a pressure of 50 kgf/cm^2. After 5 min, the melt specimens were cooled by cold compression at 50 kgf/cm^2 for 2 min, and then removed from the mold.

A tensile mechanical test was performed according to the ASTM D638 standard. Type-V dumbbell-shaped specimens were used, and the tests were performed using Shimazu AGS-2000G at a constant cross-rate of 1 mm/min at room temperature. The tensile strength, tensile modulus and elongation at break were obtained from the stress–strain curve, and the tensile toughness was determined by integrating the area under the stress–strain curve. A minimum of four tests was required for each reported value.

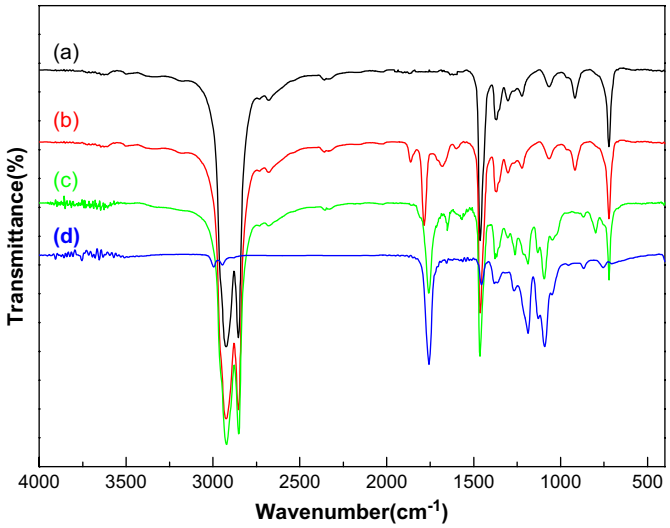

Fig. 1. FT-IR spectrum of PLA and TPO-derived copolymers (a) neat TPO; (b) maleic anhydride modified TPO; (c) TPO–PLA copolymer; (d) neat PLA.

2.7. Scanning electron microscopic observation of morphology

Scanning electron microscopy was applied to characterize the morphology of the blends. The cyro-fractured and tensile-fractured surfaces were coated with thin-layer gold, and then were scanned at an acceleration voltage of 5 kV.

3. Results and discussion

3.1. Synthesis and characterization of TPO–PLA copolymer

Different from the earlier studies adopting strict polymerization technique [17,18], TPO–PLA copolymers were herein synthesized by the esterification of terminal hydroxyl groups of PLA with the succinic anhydride groups of TPO–MAH, which were prepared by reacting maleic anhydrides with TPO-macroradicals that were formed in the presence of benzoyl peroxide as the initiator, catalyzed by DMAP. Scheme 1 displays the protocol of TPO–PLA copolymer synthesis.

Fig. 1 compares the IR spectra of neat TPO and TPO–MAH. MAH grafted onto TPO shows new absorption at 1864 cm^{-1} and 1786 cm^{-1} associated with the asymmetric and symmetric stretchings of C=O in the succinic anhydride units, respectively, and the characteristic signal at 1786 cm^{-1} corresponds to the MAH oligomeric segments in the functionalized polyolefin [21]. The inherent viscosity of TPO and TPO–MAH, presented in Table 1, shows that the molecular weight of TPO rose upon functionalization with

Table 1
Reaction recipes of TPO–MAH and TPO–PLA syntheses and their corresponding inherent viscosities

Copolymer code	Reactant recipes			Inherent viscosity
	BPO (%)	MAH (%)	DMAP (M)	(dL/g)[a]
TPO	–	–	–	0.67
TPMA06	0.5	0.25	–	0.79
TPMA13	1.0	0.50	–	0.84
TP06PL04	0.5	0.25	0.4	0.80
TP06PL08	0.5	0.25	0.8	0.87
TP06PL16	0.5	0.25	1.6	0.89
TP13PL04	1.0	0.50	0.4	0.85
TP13PL08	1.0	0.50	0.8	0.90
TP13PL16	1.0	0.50	1.6	0.96

[a] Inherent viscosity was measured at 35 °C, and the concentration was 0.5 g/dL in toluene.

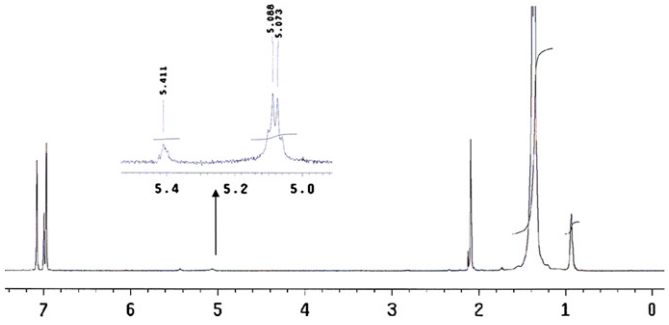

Fig. 2. ^{1}H NMR spectrum of TPO–PLA copolymer.

maleic anhydride and the M_w increased with the concentration of BPO and MAH. These results account for the occurrence of recombination of polymer chains. The degree of maleic anhydride grafted onto TPO, determined by reverse titration, increased as more BPO and MAH were used in the functionalization reaction.

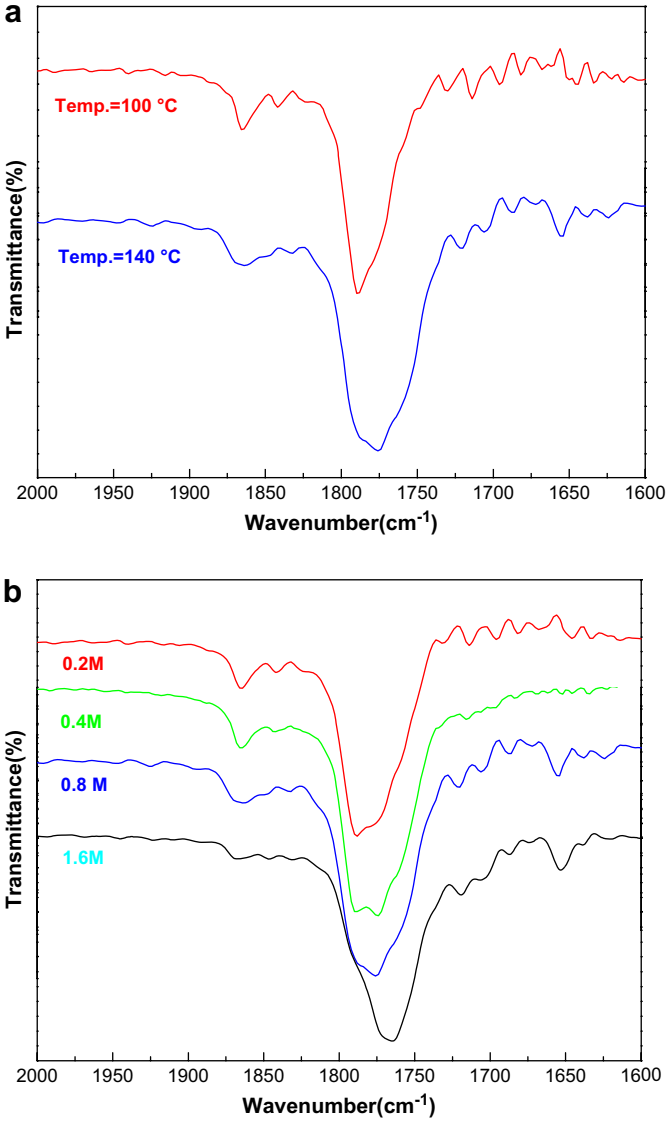

Fig. 3. FT-IR spectrum of TPO–PLA which was synthesized under various conditions (a) reaction temperature as variable; [TPO] = 10 wt%, [PLA] = 20 wt%, [DMA] = 0.8 M. (b) DMAP concentration as variable; [TPO] = 10 wt%, [PLA] = 20 wt%, reaction temp = 140 °C.

Fig. 1(c) represents the FT-IR spectrum of PLA–TPO copolymer, indicating that the absorption of anhydride units disappeared and a new absorption signal consistent with PLA carbonyl stretching appeared at 1758 cm^{-1}; a set of characteristic absorptions in the fingerprint region of 1500–1000 cm^{-1} were also present, like those of neat PLA displayed in Fig. 1(d). The methylene proton resonance of the lactide moiety at 5.1 ppm was observed in the ^{1}H NMR spectrum shown in Fig. 2, and the inherent viscosity of TPO–PLA was higher than that of TPO–MAH (Table 1). These results demonstrate that the PLA segments were successfully grafted onto TPO catalyzed by a nucleophilic catalyst.

3.2. Factors influencing the reactivity of grafting PLA onto TPO–MAH

To elucidate the effect of reaction temperature and concentration of DMAP on the reactivity of grafting PLA onto TPO–MAH, FT-IR spectra were used to analyze the relative absorption strength at 1786 cm^{-1} and 1758 cm^{-1}, which corresponds to the concentration of anhydride groups and PLA carbonyl stretching absorption in the TPO–PLA copolymer, respectively. Fig. 3(a) reveals a decline of absorption strength at 1786 cm^{-1}, a broadening of the carbonyl signal and the appearance of an absorption shoulder near 1758 cm^{-1} as the reaction temperature increased. As presented in Fig. 3(b), the

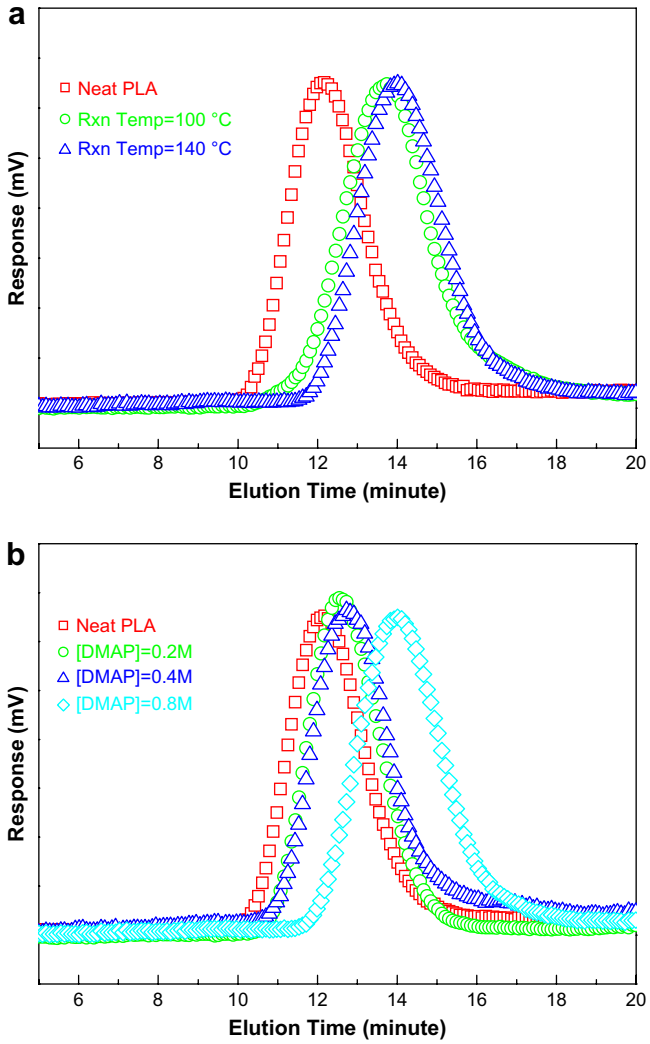

Fig. 4. PLA degradation as a function of reaction variable; (a) reaction temperature as variable; [TPO] = 10 wt%, [PLA] = 20 wt%, [DMA] = 0.8 M. (b) DMAP concentration as variable; [TPO] = 10 wt%, [PLA] = 20 wt%, reaction temp = 140 °C.

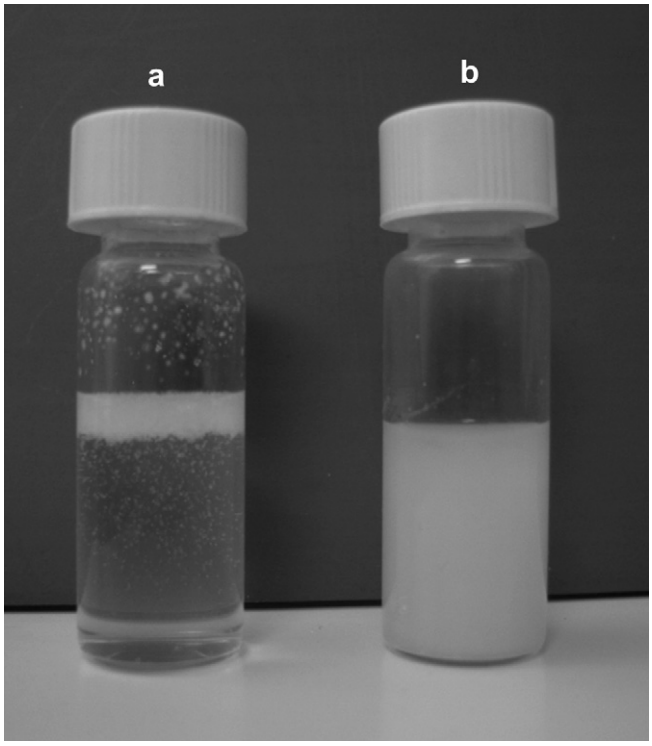

Fig. 5. Molau test of (a) PLA/TPO binary blend and (b) PLA/TPO/TPO–PLA (80/20/5) ternary blend.

intensity of absorption at 1786 cm^{-1} decreased as the DMAP concentration increased, but the PLA carbonyl absorption at 1758 cm^{-1} intensified, indicating that the graft reaction exhibited high reactivity at high temperature and DMAP concentration because more anhydride groups were consumed and more PLA segments were grafted onto TPO.

Esterification of TPO–MAH with PLA, catalyzed by DMAP, was accompanied by a transesterification reaction, which caused the depolymerization of PLA [22]. Fig. 4 shows the effects of the reaction temperature and the DMAP concentration on the M_w of PLA that was extracted from the reaction solution. The figure indicates that the rate of PLA degradation increased with the reaction temperature and that the use of more DMAP in the graft reaction would cause more severe PLA degradation. The result correlates with the reactivity of graft polymerization: a low M_w PLA is readily grafted onto TPO–MAH, because (1) the steric hindrance existing between TPO–MAH and PLA segments is reduced, (2) PLA with low M_w exhibits greater mobility and (3) formation of more terminal hydroxyl groups via depolymerization increases the grafting reaction rate. The formation of an interpolymeric network held together via dipolar association between succinic anhydride moieties [23] also hindered the graft reaction because the reactive sites were sheltered by TPO. Fortunately, the equilibrium formation of an acylpyridinium cation through the reaction of DMAP and anhydride [24], eliminating the polar aggregation and destroying the interpolymeric network structure, promoted the graft polymerization reaction.

3.3. Molau test and morphology of PLA/TPO blend

The Molau test [25] was carried out to evaluate the improvement of compatibility of PLA/TPO blends. As shown in Fig. 5, the PLA/TPO (80/20) binary blends dissolved in ethyl acetate exhibited obvious phase separation, while the blends with 5 wt% copolymer showed a milky, colloidal suspension solution in the stable state, indicating that the emulsifying function of PLA–TPO copolymer effectively stabilized the TPO particle dispersed in the PLA solution.

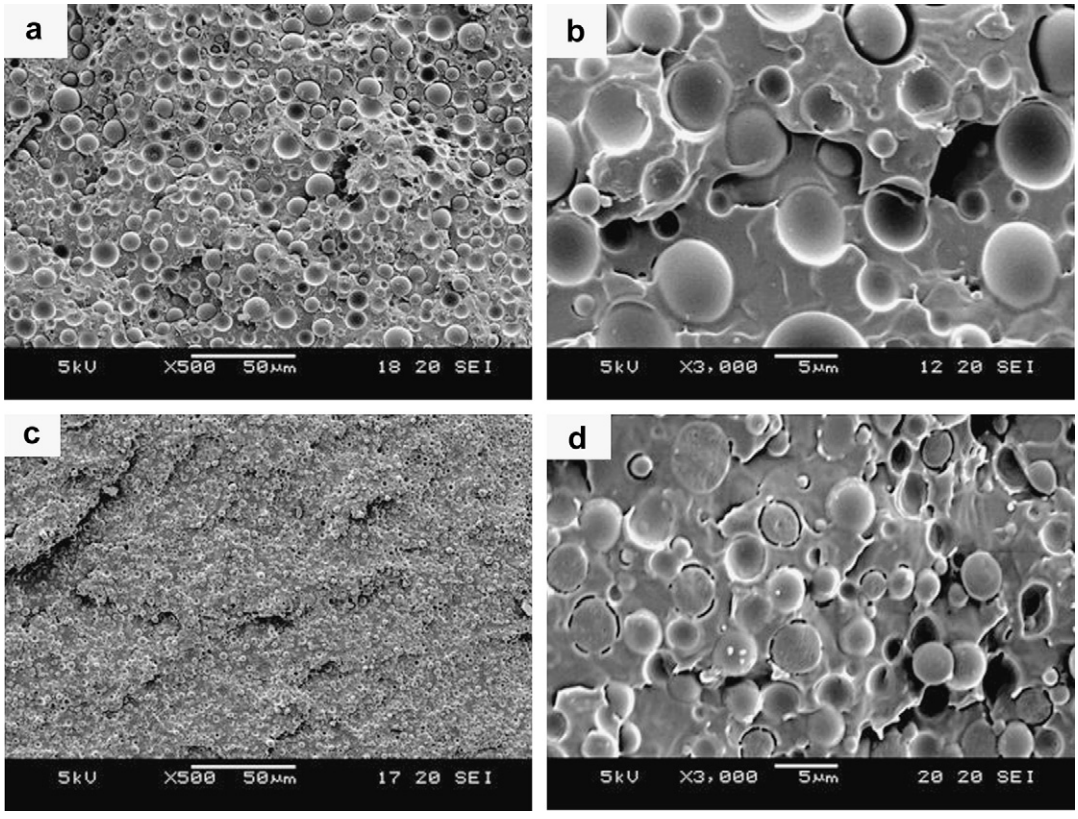

Fig. 6. Cyro-fractured surface morphology of PLA/TPO (80/20) blend: (a) without TPO–PLA, 500×; (b) without TPO–PLA, 3000×; (c) with 5 wt% TPO–PLA copolymer, 500×; (d) with 5 wt% TPO–PLA copolymer, 3000×.

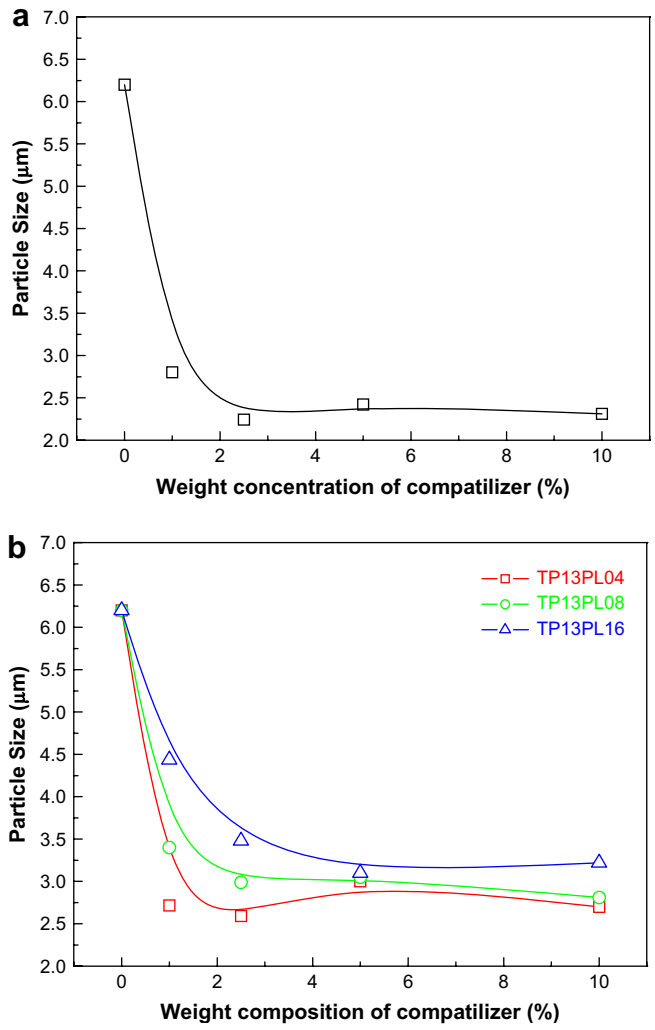

Fig. 7. Emulsification curve of PLA/TPO (80/20) blend compatibilized by various copolymers: (a) coded TP06PL08 copolymer compatibilized the PLA/TPO blend; (b) effect of DMAP concentration on the TPO particle size in the PLA matrix.

Fig 6(a–d) presents the cyro-fracture surface of PLA/TPO (80/20) blend without and with TPO–PLA copolymer. Obviously, TPO is dispersed in the PLA matrix as discrete spheres with the particle size of 6.2 μm (as determined by dynamic light scattering instrument), suggesting the strong incompatibility and weak

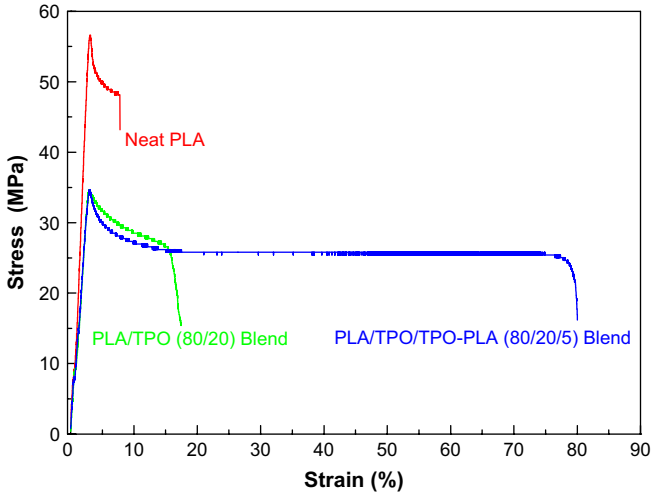

Fig. 8. Stress–strain curve of neat PLA and PLA/TPO blend.

interfacial adhesion between PLA and TPO. As can be seen, upon compatibilization of PLA/TPO(80/20) blend by adding 5 wt% TPO–PLA copolymers, the particle size of TPO dispersed in PLA matrix decreased to 2.1 μm, revealing the effective reduction of interfacial tension and the improvement of compatibility and interfacial adhesion. Fig. 7(a) shows the particle size versus the weight concentration of compatibilizers. The figure reveals that as more copolymers were added, the particle size of the TPO particles continued to decrease and then the particle size was leveled-off, because the micelles were formed beyond the critical micelle concentration that was required to saturate the interface between two immiscible polymers, and further addition of more compatibilizers would not improve the interfacial properties [26–28].

3.4. Mechanical properties of PLA/TPO blend

Fig. 8 shows the stress–strain curve of neat PLA, PLA/TPO (80/20) blend and PLA/TPO/TPO–PLA (80/20/5) blend, and Table 2 (entry 1–5) presents the detailed mechanical properties of the PLA/TPO blends with various TPO–PLA copolymer concentration. The tensile strength and tensile modulus of PLA/TPO blends were 34.7 MPa and 1.10 GPa, respectively, lower than neat PLA, as a consequence of the elastomeric nature of TPO with low strength and modulus; the elongation at break and tensile toughness were

Table 2
Mechanical properties of PLA homopolymer and PLA/TPO blends

Entry	Blend composition PLA/TPO/TPO–PLA	Compatibilizer[a]	Tensile strength (MPa)	Tensile modulus (GPa)	Elongation at break (%)	Tensile toughness (MJ/m^3)	Izod impact strength[c] (J/m)
1	100/0/0	–	54.2 ± 2.5	2.22 ± 0.50	6.0 ± 0.10	2.3 ± 0.5	73 ± 17
2	80/20/0	TP06PL08	34.7 ± 0.7	1.46 ± 0.03	15.4 ± 1.4	4.6 ± 1.0	137 ± 21
3	80/20/1.0	TP06PL08	35.6 ± 0.4	1.21 ± 0.02	99.1 ± 22.4	25.7 ± 6.3	NB[e]
4	80/20/2.5	TP06PL08	33.1 ± 0.5	1.20 ± 0.01	128.4 ± 18.2	29.9 ± 4.8	NB
5	80/20/5.0	TP06PL08	34.6 ± 0.7	1.10 ± 0.01	107.2 ± 35.4	27.4 ± 0.8	NB
6	80/20/2.5	TP06PL04	30.1 ± 1.3	1.10 ± 0.03	181.9 ± 10.1	38.5 ± 2.1	NB
7	80/20/2.5	TP06PL16	33.5 ± 0.8	1.10 ± 0.02	101.7 ± 16.5	24.7 ± 3.8	NB
8	80/20/2.5	TP13PL04	31.0 ± 0.3	1.16 ± 0.02	162.8 ± 30.2	37.1 ± 7.6	NB
9	80/20/2.5	TP13PL08	32.7 ± 0.7	1.18 ± 0.01	140.8 ± 17.9	33.1 ± 4.4	NB
10	80/20/2.5	TP13PL16	33.3 ± 0.4	1.21 ± 0.08	99.3 ± 19.3	22.9 ± 6.3	NB
11	80/20/5.0	TPMA06	32.4 ± 0.4	1.06 ± 0.02	52.2 ± 12.6	13.1 ± 3.3	NB
12	0/100/0	–	7.3[b]	NA[d]	1000[b]	NA	NA

[a] The codes of the compatibilizers used in the PLA/TPO blends were taken from Table 1.
[b] The data was received directly from the technique information released by Dow-Dupont elastomer.
[c] The unnotched-type specimens were used in the impact strength test.
[d] NA: not available.
[e] NB: samples are not break.

insignificantly improved. The SEM image of the tensile-fractured surfaces of binary blend, shown in Fig. 9(a), clearly reveals that the undeformed TPO spheres were left at the fractured surface. This result indicated that the weak interfacial adhesion associated with the incompatibility of the TPO/PLA blend couldn't bear the applied stress, which could thus not be transferred across the interface between the polymers, resulting in a limited improvement of the mechanical properties. Upon compatibilization of PLA/TPO (80/20) blends by the addition of TPO–PLA copolymers, the tensile strength and the tensile modulus remained almost on the same scale, regardless of the presence or absence of the TPO–PLA copolymer as well as the compatibilizer concentration, because the interfacial adhesion level has no influence on the low-strain tensile properties [29]. Nevertheless, the tensile toughness and elongation at break increased to 29.9 MJ/m^3 and 128%, respectively, with the concentration of the compatibilizers, but deceased when 5 wt% of TPO–PLA copolymer was used because adding more compatibilizers beyond the CMC often worsens the overall performance of the blend material. [27] The fractured morphology of the ternary blend, distinctly different from that in Fig. 9(a), exhibited considerable ductile tearing, surface roughness and absence of sphere particles at the fractured surface, suggesting that the crack propagation absorbed considerable strain energy before failure [30] and the TPO–PLA copolymers increased the interfacial adhesion between PLA and TPO phases, leading to a significant improvement of toughness of PLA.

3.5. Effect of chemical structure of compatibilizers on mechanical properties

As described in the literature [11,31,32], the copolymer architecture affects the compatibilization efficiency of a compatibilizer in the polymer blends. In this section, a set of compatibilizers were synthesized by altering the concentration of BPO, MAH and DMAP and the effects of chemical structure and the composition on the mechanical properties were discussed. The codes for the copolymers in Table 1 were expressed based on the MAH-graft level (%) and the DMAP concentration used in the graft reaction. Table 2 (entry 6–10) presents the mechanical properties of the PLA/TPO blend with 2.5 wt% compatibilizers. The tensile strength and tensile modulus were almost the same in those ternary blend system for the same reason mentioned in the preceding section; however, the concentration of DMAP seems to dominate the improvement of elongation at break (%) and tensile toughness, but the graft level (%) has slight effect on the property. The plot of particle size versus compatibilizer concentration shown in Fig. 7(b) indicates that reducing the amount of DMAP used in the graft reaction leads to smaller equilibrium particle size and that the aggregation of dispersed particle is more effectively suppressed.

With respect to the effect of DMAP concentration on the chemical composition of the TPO–PLA copolymers, the M_w of the PLA segment grafted onto TPO–MAH could be adjusted and controlled in a single step procedure using a nucleophilic catalyst, such as DMAP, via the depolymerization of PLA [22]. As described in the previous section, using more DMAP in the graft reaction yields a PLA with lower M_w, such that the compatibilizer with longer PLA moieties was synthesized when less DMAP was added. Moreover, as described elsewhere [31], the surface coverage of the graft copolymer increased with the length of the graft chain because of the strong repulsive interaction ε_{AB} between the constitutive segments in the graft copolymer. As a result, the copolymers are located at the interface rather than in the matrix or in the dispersed phase, improving the miscibility of the immiscible polymer blends. Hence, the TPO–PLA copolymers with longer PLA chains show more efficiency in the compatibilization of the PLA/TPO blend [9,11], and exhibit significant chain entanglement between the polymer phases, which prevents copolymers from being pulled out from the interface and improves the mechanical properties of the PLA/TPO blends.

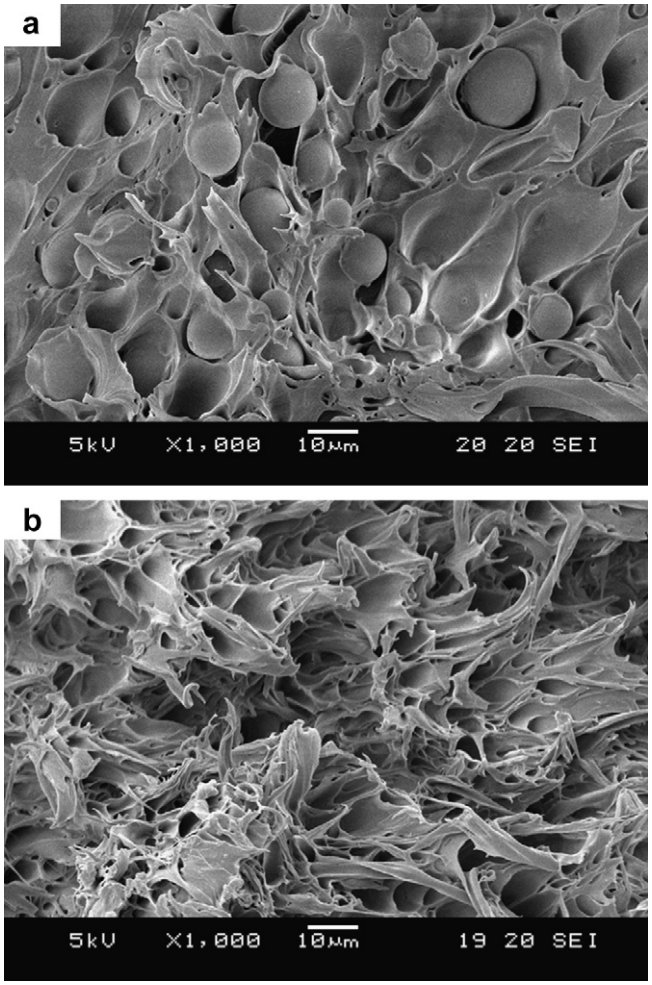

Fig. 9. SEM of tensile-fractured surface of PLA/TPO (80/20) blends: (a) without TPO–PLA copolymer; (b) with 5 wt% TPO–PLA copolymer.

3.6. Comparison of TPO–MAH as compatibilizer with TPO–PLA

In previous studies [13–15,26], TPO–MAH has been adopted as a compatibilizer to promote the compatibilization of polyester/TPO blends. In this final section, two compatibilizers, TPO–MAH and TPO–PLA synthesized in our laboratory, were applied to compatibilize PLA/TPO blends and the improvements in the compatibility and the mechanical properties of the PLA/TPO blends were compared. All of the blends were prepared with 80 wt% of PLA, 20 wt% of TPO and 5 wt% of compatibilizers. TPO–MAH, used as a compatibilizer and a precursor for the synthesis of TPO–PLA copolymers, was taken from the same batch. Figs. 10 and 11 show the SEM images of cyro-fractured surface and a particle size analysis of PLA/TPO blends with various compatibilizers, respectively. TPO–MAH and TPO–PLA both enhanced the compatibility of the PLA phase and the TPO phase: TPO particle size was 5.1 μm in TPO–MAH but only 2.1 μm in TPO–PLA. Additionally, a narrower particle size distribution was observed in the PLA/TPO/TPO–PLA blend system. Table 2 (entries 5 and 11) presents the mechanical testing results. Upon addition of these two compatibilizers, the two blends both exhibited a higher elongation at break and tensile toughness than those of neat PLA. However, the rare formation of copolymer *in situ*

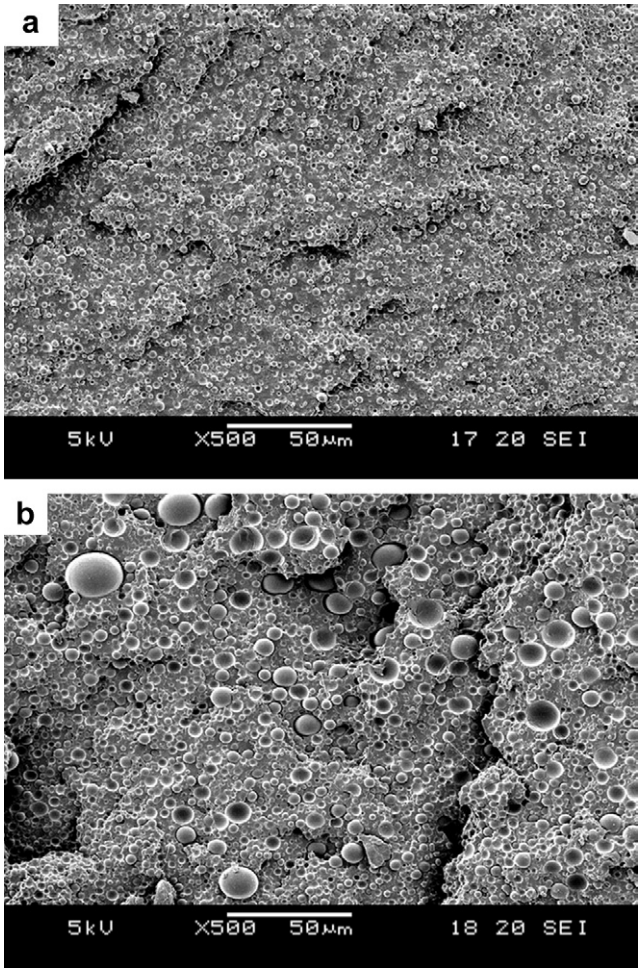

Fig. 10. Cyro-fractured surface morphology of PLA/TPO (80/20) blends compatibilized by various compatibilizers: (a) 5 wt% TPO–PLA copolymer; (b) 5 wt% TPO–MAH copolymer.

during melt blending in the PLA/TPO/TPO–MAH blend, leading to less chain entanglement at the interface between two polymer phases, exhibits worse elongation at break and tensile toughness, as compared with the PLA/TPO/TPO–PLA blend. These results indicate that the TPO–PLA copolymer is more efficient in reducing the interfacial tension and enhancing the compatibility of PLA/TPO blends than TPO–MAH.

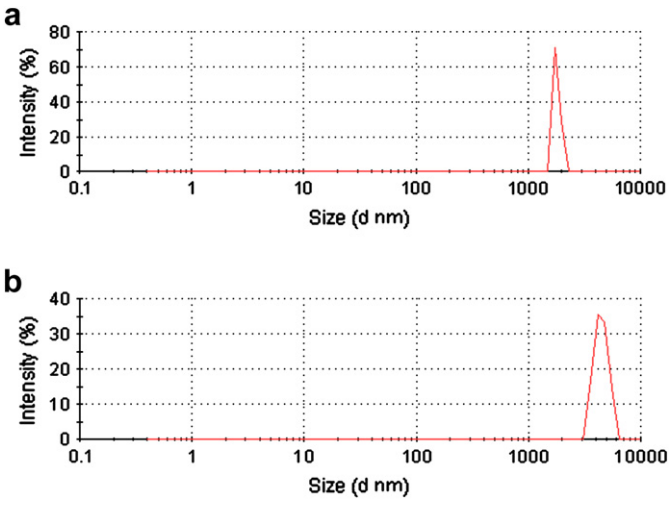

Fig. 11. Particle size distribution of PLA/TPO blends compatibilized by various compatibilizers: (a) 5 wt% TPO–PLA copolymer; (b) 5 wt% TPO–MAH copolymer.

4. Conclusion

TPO–PLA copolymers were synthesized by the esterification of maleic anhydride functionalized thermoplastic polyolefin elastomer (TPO–MAH) with polylactide in the presence of 4-dimethylaminopyridine. The nucleophilic catalyst, causing depolymerization of PLA via transesterification and reducing the intermolecular interaction in TPO–MAH, effectively increases the reactivity of PLA-graft reaction with the reaction temperature and DMAP concentration because of the substantial elimination of the steric hindrance effect. A Molau test and the SEM images of cyro-fractured surface of PLA/TPO binary blends and PLA/TPO/TPO–PLA ternary blends, which are prepared by melt blending in a Brabender mixer, indicated that the particle size dispersed in PLA matrix substantially decreased as the concentration of the compatibilizers increased, until the content exceeded the critical micelle concentration. Compatibilizing the PLA/TPO (80/20) blend with TPO–PLA copolymer reduced the tensile strength and tensile modulus because of the natural elastic property with low strength and modulus; however, the enhanced interfacial adhesion strength markedly increased the elongation at break and tensile toughness, which however, slightly decreased when 5 wt% compatibilizers were added because of the formation of micelle that would worsen the performance of blend system. The ternary blends that were compatibilized by TPO–PLA copolymers with long PLA segments exhibited higher elongation at break and tensile toughness, because the compatibilizer shows strongly repulsive interaction between the constitutive segments in the copolymer, increasing the surface coverage and chain entanglement at the interface. Comparing TPO–PLA with TPO–MAH as a compatibilizer indicated that a TPO–PLA copolymer is more efficient in compatibilizing the PLA/TPO (80/20) blend; it is associated with the smaller particle size, narrower size distribution and higher elongation at break and greater tensile toughness.

Acknowledgements

The authors would like to thank the Industrial Technology Research Institute of Taiwan, ROC, for financially supporting this research.

Appendix. Supplementary data

Supplementary data associated with this article can be found in the online version, at doi:10.1016/j.polymer.2008.06.054.

References

[1] Drumright RE, Gruber PR, Henton DE. Adv Mater 2000;12(23):1841–6.
[2] Auras R, Harte B, Selke S. Macromol Biosci 2004;4(9):835–64.
[3] Joziasse CAP, Veenstra H, Grijpma DW, Pennings AJ. Macromol Chem Phys 1996;197(7):2219–29.
[4] Grijpma DW, Penning JP, Penmings AJ. Colloid Polym Sci 1994;271(9):1068–81.
[5] Li YJ, Shimizu H. Macromol Biosci 2007;7(7):921–8.
[6] Noda I, Satkowski MM, Dowrey AE, Marcott C. Macromol Biosci 2004;4(3):269–75.
[7] Anderson KS, Lim SH, Hillmyer MA. J Appl Polym Sci 2003;89(14):3757–68.
[8] Lu JM, Qiu ZB, Yang WT. Polymer 2007;48(14):4196–204.
[9] Zhang CL, Feng LF, Gu XP, Hoppe S, Hu GH. Polymer 2007;48(20):5940–9.
[10] Kim J, Zhou HY, Nguyen ST, Torkelson JM. Polymer 2006;47(16):5799–809.
[11] Dıaz MF, Barbosa SE, Capiati NJ. Polymer 2007;48(4):1058–65.
[12] Bhattacharyya AR, Ghosh AK, Misra A, Eichhorn KJ. Polymer 2005;46(5):1661–74.
[13] Guerrica-Echevarria G, Eguiazabal J, Nazabal J. Eur Polym J 2007;43(3):1027–37.
[14] Aróstegui A, Nazábal J. Polymer 2003;44(1):239–49.
[15] Chapleau N, Huneault MA. J Appl Polym Sci 2003;90(11):2919–32.

[16] Huang J, Paul DR. Polymer 2006;47(10):3505–19.
[17] Wang YB, Hillmyer MA. J Polym Sci Part A Polym Chem 2001;39(16):2755–66.
[18] Schmidt SC, Hillmyer MA. Macromolecules 1999;32(15):4794–801.
[19] Shi D, Yang JH, Yao ZH, Wang Y, Huang HL, Jing W, et al. Polymer 2001;42(13):5549–57.
[20] Jiang CH, Filippi S, Magagnini P. Polymer 2003;44(8):2411–22.
[21] Qiu WL, Hirotsu T. Macromol Chem Phys 2005;206(24):2470–82.
[22] Nederberg F, Connor EF, Glausser T, Hedrick JL. Chem Commun 2001;20:2066–7.
[23] Zhang MZ, Dhuamel J, van Duin M, Meessen P. Macromolecules 2004;37(5):1877–90.
[24] Xu SJ, Held I, Kempf B, Mayr H, Steglich W, Zipse H. Chem Eur J 2005;11(16):4751–7.
[25] Molau GE. J Polym Sci Part A Polym Chem 1965;3(4):1267–78.
[26] Aravind I, Albert P, Ranganathaiah C, Kurian JV, Thomas S. Polymer 2004;45(14):4925–37.
[27] Mathew M, Thomas S. Polymer 2003;44(4):1295–307.
[28] Joseph S, Laupretre F, Negrell C, Thomas S. Polymer 2005;46(22):9385–95.
[29] Aróstegui A, Nazábal J. Polymer 2004;44(18):5227–37.
[30] Bhardwaj R, Mohanty AK. Biomacromolecules 2007;8(8):2476–84.
[31] Park JS, Kim HC, Jo WH. Polym Bull 1998;40(4–5):607–12.
[32] Zhu YT, Ma ZW, Li YQ, Cui J, Jiang W. J Appl Polym Sci 2007;105(3):1591–6.